SWIMMING SPEED DISTRIBUTIONS OF BULL SPERMATOZOA AS DETERMINED BY QUASI-ELASTIC LIGHT SCATTERING

F. R. HALLETT, T. CRAIG, AND J. MARSH, *Department of Physics, University of Guelph, Guelph, Ontario N1G2W1, Canada*

ABSTRACT 88 semen samples from 39 bulls have been investigated by the quasi-elastic light scattering technique. Normal, defective, and dead cells each yielded characteristic autocorrelation functions. The form of these functions indicates that the swimming speed distribution of normal cells is a gamma distribution with two degrees of freedom while that for defective or circular swimmers is a gamma distribution with one degree of freedom. The resulting analysis of the experimental autocorrelation functions yields the fraction of the sample that is normal, the fraction that is defective, and the average speed of each group. The average helical swimming speed of normal cells was found to be 384 μm/s, while the average trajectory speed of the circular swimmers was found to be 103 μm/s. The overall quality of each of the semen samples as determined by light scattering is compared to quality determination on the same samples by technicians from the artificial insemination industry.

INTRODUCTION

In recent years considerable effort has been made to determine spermatozoal viability and motility quantitatively with the quasi-elastic light scattering technique. Much of the work was precipitated by the appearance of a paper by Nossal (1971), in which the frequency spectra and the electric field autocorrelation functions were predicted for selected hypothetical swimming speed distributions. The experimental and theoretical investigations were mostly of motile bacteria (Nossal et al., 1971; Nossal and Chen, 1972, 1973; Schaefer, 1973; Berne and Nossal, 1974; Boon et al., 1974; Schaefer and Berne, 1975; Chen et al., 1977). The published results on spermatozoa are principally those of a French group (Adam et al., 1969; Dubois et al., 1975; Jouannet et al., 1977), but other contributions have been made by Cooke et al. (1976) and by Shimizu and Matsumoto (1977). Several other groups have studied spermatozoal preparations, but have not published their results.

The difficulties in these experiments have been due to both experimental and theoretical uncertainties. The experimental uncertainty arises from the extreme variability in the quality of samples. This variability, we have found, is due not only to sample handling procedures but to variability in the quality of raw semen and the collection procedures followed as well. As will be demonstrated, this variability makes accurate scattering vector dependence experiments quite difficult. This in turn leads to theoreti-

cal uncertainties as to whether or not the wiggling motion of the spermatozoa influences the shape of the observed autocorrelation functions and frequency spectra.

In this paper we will provide further evidence that light scattering does provide reliable estimates of the swimming properties of spermatozoal populations. The sizeable variability in the shape of the experimental autocorrelation functions observed by ourselves and others appears to be due to the presence, in varying amounts, of defective or circular swimmers in the sample. The form of the autocorrelation function of these defective swimmers is given, together with those of normal and dead cells. The corresponding speed distributions of normal and defective cells are found to be gamma distributions with two and one degrees of freedom, respectively. It will also be shown that the expected scattering vector dependence is different for autocorrelation functions from normal, defective, and dead cell populations. This provides one possible explanation of the difficulty of observing similar scattering vector dependencies in experiments on different samples.

Although we present average values for the fraction normal, the fraction defective, and their respective swimming speeds, these values must be considered as tentative until the scattering vector studies are complete. Work by Shimizu and Matsumoto (1977) has indicated that the autocorrelation functions from boar and abalone spermatozoa do scale as expected for normal swimmers. We have not yet, however, confirmed the scattering vector dependence for bull spermatozoa populations. Nevertheless the relative values of the parameters are still meaningful and one may, on this basis, compare samples.

METHODS

The quasi-elastic light scattering apparatus used in this study is similar to others described in the literature (Berne and Pecora, 1976). In our case the beam from a Jodon 15 mW helium neon laser (Jodon Engineering Associates, Inc., Ann Arbor, Mich.) was focused into a scattering chamber thermally regulated at 30 ± 0.5°C. The light scattered from the sample was collimated by two 400-μm pinholes set to obtain a scattering angle of 15°. The light was detected by an RCA 8852 photomultiplier (RCA Solid State, Somerville, N.J.). The photocounts from the photomultiplier were fed into an amplifier discriminator (model 1140 quantum photometer, Princeton Applied Research Corp., Princeton, N.J.) and then to an interface to a Nova-2 minicomputer (Data General Corp., Southboro, Mass.). The details of this interface and the autocorrelation process are described elsewhere (Gray et al., 1975).

To investigate a large number of samples under the best possible conditions, the apparatus was moved to the processing laboratory of United Breeders Inc. of Guelph, Ont. Data from 88 semen samples from 39 bulls were accumulated over a 10-day period. Each sample was collected by a professional with the most up-to-date methods utilized by the industry. All collection vessels, glassware, and diluting fluids were sterile and prewarmed to 30°C. As is the usual procedure in the semen processing industry, all fluorescent lights near the processing area were extinguished while samples were being prepared. Our standard procedure was to dilute 0.1 ml of the fresh semen by a factor of 2,500 with Hanks' Balanced Salt Solution (Grand Island Biological Company, Inc., Grand Island, N.Y.) and to begin data accumulation within 15 min of collection. Typically, a million photocounts were obtained from each sample, although this changed slightly depending on the concentration of spermatozoa in the prepara-

tion. The sampling interval was usually 120 μs. Total run-time for each experiment was approximately 15 min, including autocorrelation.

THEORY

Our approach to the analysis of the intensity autocorrelation functions from spermatozoal preparations has essentially been a pragmatic one of applying the various theories developed over the years and determining which best fits the data. The simplest expression for the normalized electric field autocorrelation function, $(g^{(1)}(\tau))$, is obtained if the motile particles are assumed to be point sources moving at constant velocities for times which are long with respect to the decay times of the observed functions. In such a case $g^{(1)}(\tau)$ is given by Nossal and Chen (1972) as

$$g^{(1)}(\tau) = 4\pi \int_0^\infty \frac{\sin(kv\tau)}{kv\tau} P_s(v)\, dv. \tag{1}$$

In this expression $P_s(v)$ is the speed distribution function of the scatterers, k is the scattering vector, and τ is delay time. The normalized function, $g^{(1)}(\tau)$, can be obtained from the experimental intensity autocorrelation function, $C_I(\tau)$, via

$$g^{(1)}(\tau) = A(C_I(\tau) - B)^{1/2}, \tag{2}$$

where B is an experimental background corresponding to the square of the average light intensity and A is a normalization constant.

Spermatozoa swim normally in an approximately helical path whose pitch is roughly 10 μm. The time taken to progress one cycle of the helix is about 0.1 s. Typical experimental functions of $g^{(1)}(\tau)$ from good motile samples (e.g. Fig. 1) have decay times of about 3 ms. Over these times the cell will have progressed only about $\frac{1}{30}$ of a cycle. Calculations demonstrating that the helical motion is unimportant at scattering angles greater than 1° have also been given by Combescot (1970). The requirement that velocities remain constant over times which are long with respect to decay times therefore appears to be satisfied.

However, spermatozoa are certainly not point sources. Even if scattering is assumed to arise predominantly from the head region alone, one is still considering a particle whose dimensions correspond to several wavelengths of the laser light. Thus diffraction effects are to be expected in light scattered from various parts of the same particle. Systems of this kind have been considered by Berne and Nossal (1974). They derive the expression

$$g^{(1)}(\tau) = \int_0^\infty dv \int_{-1}^{1} \frac{d\eta}{2} e^{ikv\tau\eta} e^{-\Delta\sigma^2 k^2 \eta^2} P_s(v) \Big/ \int_{-1}^{1} \frac{d\eta}{2} e^{-\Delta\sigma^2 k^2 \eta^2}, \tag{3}$$

where $\eta = \hat{k} \cdot \hat{v}$ is the cosine between $\mathbf{k}$ and $\mathbf{v}$ and $\Delta\sigma^2 = \sigma_{\|}^2 - \sigma_{\perp}^2$ reflects the deviations in the particle shape from the spherically symmetric case. Setting $\Delta\sigma^2 = 0$ in Eq. 3 leads to Eq. 1. While a spermatozoan head is not the elliptical shape used for the derivation of Eq. 3, we thought that an effective $\Delta\sigma^2$ might give us a qualitative

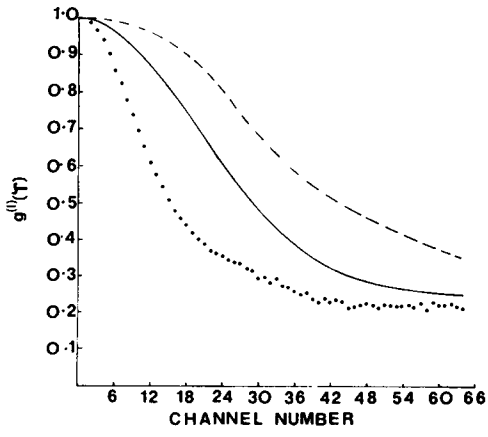

FIGURE 1

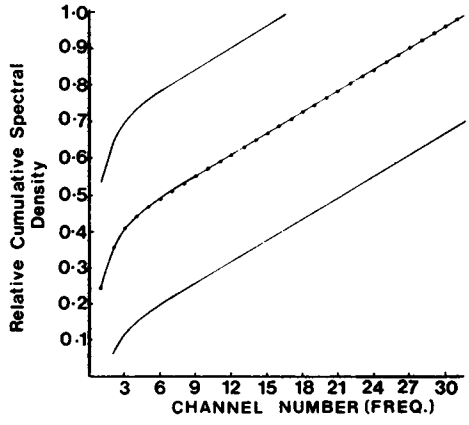

FIGURE 2

FIGURE 1 Experimental electric field autocorrelation function from a sample containing mostly normal swimmers (dots) and predicted functions using $<v_N>$ = 200 μm/s in Eq. 3 for $\Delta\sigma^2 = 0$ (solid line) and $\Delta\sigma^2 = 0.2$ (broken line).

FIGURE 2 Relative cumulative periodogram for experimental and best-fit frequency spectra using f_{NL} in Eq. 9. Dots are cumulative experimental points. The solid lines are the best-fit cumulative spectrum and the Kolmogorov-Smirnov limits.

idea as to whether or not this parameter was important. The effect of increasing $\Delta\sigma^2$ in the equation is to increase the decay time. A normal distribution of speeds as suggested by Berne and Nossal (1974) for *Escherichia coli* preparations has the form

$$P_s(v) = (3/2\pi < v_N^2 >)^{3/2} v^2 e^{-3v^2/2<v_N^2>}, \quad (4)$$

where $<v_N^2>$ refers to the mean square speed of normal cells. Assuming a value of about 200 μm/s for the root mean square speed of normal spermatozoa leads to the autocorrelation functions shown in Fig. 1 for $\Delta\sigma^2 = 0$ μm^2 and $\Delta\sigma^2 = 0.2$ μm^2. It is clear that if the experimental function shown in the figure is to be fit, then $\Delta\sigma^2$ must be very nearly zero. As will be shown later, the values for the average swimming speeds of normal cells as determined by least squares fits are quite high, about 350 μm/s. While the significance of this will be discussed later, the point now is that nonzero values of $\Delta\sigma^2$ would drive these values even higher. Consequently we have used Eq. 1 to analyze all of the experimental electric field autocorrelation functions from all semen samples.

If one has an analytical form for $P_s(v)$, it is possible by Fourier inversion of Eq. 1 to predict the appropriate form of $g^{(1)}(\tau)$. Any number of distributions are possible for $P_s(v)$. The distribution given by Eq. 4 leads to the function,

$$f_{NG} = e^{-k^2\tau^2<v_N^2/6>}, \quad (5)$$

where f_{NG} refers to the Gaussian-shaped autocorrelation function for normal helical swimmers. Cooke et al. (1976) noticed that their experimental functions were fit by an

equation of the form

$$g^{(1)}(\tau) = \alpha(f_N) + (1 - \alpha)(f_d), \tag{6}$$

where α represents the fraction of normal swimmers, f_N is scattering function for normal swimmers, which they replaced by the Lorentzian function

$$f_{NL} = \frac{1}{1 + (k\langle v_N\rangle\tau/2)^2}, \tag{7}$$

and f_d was a fourth-order polynomial that represented the scattering function from dead cells. The function f_d falls off very slowly with time and corresponds to the "apparent" background of most experimental functions (see Fig. 1). The speed distribution obtained by Fourier inversion of f_{NL} is

$$P_s(v) = (v/\pi\langle v_N\rangle^2)e^{-2v/\langle v_N\rangle}, \tag{8}$$

a gamma distribution with two degrees of freedom (Breiman, 1973).

Our reasons for analyzing a large number of semen samples from several different bulls was to determine statistically which of f_{NG} or f_{NL}, when used for f_N in Eq. 6, gave better fits to the data. Previous studies (Cooke et al., 1976) had favored f_{NL}, but these used a small number of semen samples, all from the same bull. Furthermore, collections which by microscopic inspection contained noticeable fractions of defective or circular swimmers were rejected immediately by the technicians. None of the samples at United Breeders were rejected and most contained noticeable numbers of defective swimmers. It quickly became apparent that the presence of these defective swimmers changed the shape of the electric field autocorrelation function, and further that Eq. 6 alone, using either f_{NL} or f_{NG}, was incapable of giving us good fits. Because of this a new term was added to Eq. 6 to obtain

$$g^{(1)}(\tau) = \alpha(f_N) + \beta(f_c) + (1 - \alpha - \beta)f_d, \tag{9}$$

where f_c represents the scattering function for defective or circular swimmers. Fortunately, certain samples contained substantially more circular swimmers than normal swimmers. Analysis of functions from these samples yielded the surprising result that neither Lorentzian nor Gaussian functions for f_c gave good fits. The experimental function was less flattened at the top than either of these functions and decayed more slowly. This implied (*a*) that neither Eq. 4 nor 8 described the swimming speed distribution of circular swimmers or (*b*) that other motion, such as wobble, was affecting the shape of the function. Since circular swimmers move more slowly than normal swimmers, the second possibility, an effect due to wobble, was rejected. The only speed distribution function we could find that yielded the proper-shaped scattering function was a gamma distribution with one degree of freedom;

$$P_s(v)_c = (1/4\pi\langle v_c\rangle)\, e^{-v/\langle v_c\rangle}, \tag{10}$$

which when transformed yields a scattering function for defectives of

$$f_c = (1/k\langle v_c\rangle\tau)\cot^{-1}(1/k\langle v_c\rangle\tau). \tag{11}$$

This function and either f_{NL} or f_{NG} were used in the least squares fitting of Eq. 9 to all experimental functions.

The scattering vector dependence of f_c and of f_{NL} or f_{NG} are similar in that their widths all scale inversely with k. However, the slope of the k dependence of f_c differs from the corresponding slope of f_{NL} or f_{NG} because of the presence of the inverse cotangent. The problem is further complicated by the inverse k^2 dependence of the width of f_d. Thus it is exceedingly difficult to find two samples which show identical scattering angle dependence. However, knowing α, $<v_N>$, β, and $<v_c>$ would allow one to predict the electric field autocorrelation function at any angle and compare it to the experimentally determined function. These experiments have to be carried out sufficiently rapidly so that all parameters remain unchanged over experiments at several scattering angles. Such experiments are being attempted in our laboratory at the present time.

LEAST SQUARES FITTING TECHNIQUES AND QUALITY OF FIT DETERMINATION

The generalized least squares fitting routine used in this study was acquired from the University of Waterloo Computing Centre and is based on an algorithm developed by Powell (1965). All fitting was done on the same Nova-2 minicomputer used to collect data. Four parameters, α, β, $<v_N>$, and $<v_c>$, were determined from the best fit to the 64-channel experimental function, $g^{(1)}(\tau)$. There was some tendency for the fit routine to find a local minimum, but this was easily discovered by visual examination of the fit. A new set of starting parameters always corrected the problem.

It is very difficult to determine statistically the quality of fit to an autocorrelation function because of correlated errors arising between points of the function. To circumvent this problem it is more convenient, by means of the Wiener-Khintchine theorem, to obtain the spectral density function $I(\omega)$, which has independent error on each point. Once the discrete spectral density function is obtained, it is possible to obtain the cumulative spectrum or periodogram. One may assess the deviations of the experimental periodogram, $F(x)_{\text{data}}$, (obtained from the transformed experimental functions) from the theoretical periodogram, $F(x)_{\text{theor}}$ (obtained from the transformed best fit function) by means of the Kolmogorov-Smirnov test (Box and Jenkins, 1970). This test places limits about the theoretical points such that if the function was a good estimate of the real data, then only a stated small percentage of the points of the experimental periodogram would fall outside these limits. The general approach is to assume that the model correctly predicts the data and then attempt to prove otherwise. If the statistic, D, where

$$D = \max_x | F(x)_{\text{data}} - F(x)_{\text{theor}} | \tag{12}$$

lies outside the limits given by $K_\epsilon q^{-1/2}$, where K_ϵ is the tabulated value of the D statistic at the ϵ significance level, and $q = (n - 2)/2$ for n even or $(n - 1)/2$ for n odd, n being the original number of data points, then the theoretical function is said to be a bad fit to the data with probability $1 - \epsilon$ (Winkler and Hays, 1975). For $n = 64$ the

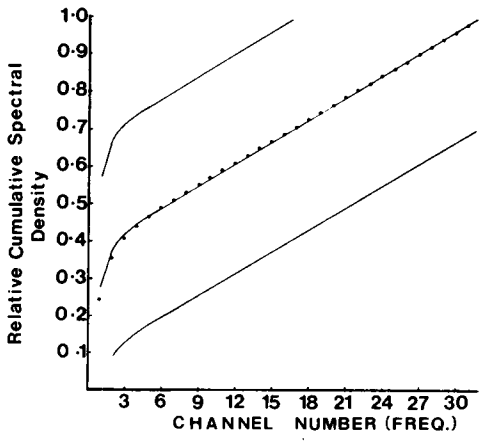

FIGURE 3

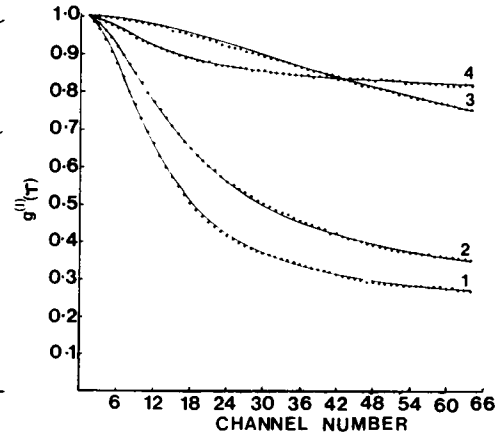

FIGURE 4

FIGURE 3 Relative cumulative periodogram for experimental and best-fit frequency spectra using f_{NG} in Eq. 9. Dots are cumulative experimental points. The solid lines are the best-fit cumulative spectrum and the Kolmogorov-Smirnov limits.

FIGURE 4 Four different experimental electric field autocorrelation functions and best-fits using f_{NL} in Eq. 9 from four samples. Fit-parameters are given in Table IV.

limits are $\pm 1.63/\sqrt{31}$ or 0.29 with $\epsilon = 0.01$. Figs. 2 and 3 show periodograms that result from both Lorentzian and Gaussian fits to data from a sample which appeared both visually and experimentally (Fig. 4, curve 1), to be of high quality. That is, in this sample almost all cells were swimming normally. While both f_{NL} and f_{NG} give reasonable fits to the experimental function and yield similar values for α and $<v_N>$ (see Table I), close inspection of the periodograms indicates that f_{NL} is superior. When the Gaussian function was used the final values of β and $<v_c>$ were higher than one would expect for such a high-quality sample. In addition the sum of squares of differences between the data and the fit function was consistently a factor of 10 or more lower when f_{NL} was used. Thus, while f_{NL} may not be the perfect function describing the scattering function from normal swimmers, the true function is certainly very close to it. All analysis of data leading to the results in the following section was done using f_{NL}.

The uncertainties associated with the four fit parameters were examined, again using

TABLE I

FIT PARAMETERS USING f_{NL} OR f_{NG} IN EQ. 9

Parameter	f_{NL}	f_{NG}
α	0.75	0.63
$<v_N>$, $\mu m\, s^{-1}$	370	350
β	0.0	0.25
$<v_c>$, $\mu m\, s^{-1}$	0.0	63
Sum of squares	6.6×10^{-4}	3.1×10^{-2}

the spectral density functions. If $I_i(\omega)$ were $i = 1, N$ points is the experimental spectral density function then

$$I_i'(\omega) = f_i(m_1, m_2, \ldots m_k) + e_i \tag{13}$$

is the corresponding transformed, best-fit function consisting of parameters $m_1, \ldots m_k$. Each point, i, has an associated error e_i normally distributed with mean of zero and variance of σ^2. An estimate of this variance is given by Box and Jenkins (1970) as

$$\hat{\sigma}^2 = S/(n - k), \tag{14}$$

where

$$S = \sum_{i=1}^{n} (I_i(\omega) - f_i(m_1, \ldots m_k))^2. \tag{15}$$

The effect of changing the parameters on $I_i'(\omega)$ may be obtained using the linearization procedure (Baird, 1962);

$$\partial I_i'(\omega) = (\partial f_i/\partial m_j)\, \partial m_j + \cdots + e_i, \tag{16}$$

which can be converted to a matrix equation:

$$Y = X b + e, \tag{17}$$

where X is an n-by-k matrix of the derivatives. The range in values of the parameters that will result in equally good fits is then given by (Box and Jenkins, 1970):

$$(m - \hat{m})'(X'X)(m - \hat{m}) \leq \chi_\epsilon^2(n - k)\, \hat{\sigma}^2, \tag{18}$$

where the prime indicates the transpose of a matrix and $\chi_\epsilon^2(n - k)$ is the value of the chi-square function at the ϵ significance level for $n - k$ degrees of freedom. This equation defines an ellipse in k-dimensional space whose shape measures the range of values of the parameters at a $(1 - \epsilon) \times 100\%$ confidence level. The ranges of the parameters can be more readily expressed through the covariance matrix (Searle, 1971),

$$\operatorname{cov}(\delta m) = \hat{\sigma}[(X'X)^{-1}], \tag{19}$$

the main diagonal elements of which are the estimated variance of each of the parameters. If these variances are multiplied by the value of Student's t distribution for $n - k$ degrees of freedom at the 0.05% significance level (i.e. $t_{0.995,(n-k)}$), the result is an error on each of the parameters at the 1% level of significance or, equivalently, the 99% confidence level. Thus

$$m_k = \hat{m}_k + \hat{\sigma}[(X'X)^{-1}]_{kk}^{1/2}\, t_{0.995,(n-k)}. \tag{20}$$

Examples of the absolute errors in the parameters are shown in Table II for the fit parameters given in Table I. The error on α was about 1% when f_{NL} was used as the scattering function for normal cells. Similar errors on α were observed when the sample contained mostly normal cells. When samples contained sizeable fractions of de-

TABLE II

ESTIMATED ABSOLUTE ERRORS IN PARAMETERS USING f_{NL} OR f_{NG} IN EQ. 9

Parameter	f_{NL}	f_{NG}
α	0.007	0.15
$<v_N>$	0.003	0.002
β	0.001	0.014
$<v_c>$	0.00001	0.0002

fective swimmers the errors on α were about 5%. The error on α was quite large, about 20%, in two circumstances rarely encountered. The first was when α was very small (< 0.1) and the second occurred when the defective swimmers were nearly as active as the normal swimmers. In the latter case the widths of the normal and defective scattering functions were similar and the fits were, therefore, less certain.

The listed absolute errors on the other parameters should not be viewed independently from the error on α. This is because of the sizeable correlations between the parameters.

It is possible to obtain some insight into the amount of correlation between parameters by calculating the correlation matrix (Searle, 1971);

$$\text{corr}(\delta m)_k = \frac{\text{cov}(\delta m)_{kl}}{(\text{cov}(\delta m)_k \text{cov}(\delta m)_l)^{1/2}}, \tag{21}$$

where l is an index of the parameters as is k. This matrix has diagonal elements of unity (i.e. when $l = k$) and off-diagonal elements of zero for totally uncorrelated parameters. As the correlation between parameters increases, these elements approach $+1$ or -1, depending on whether the correlation is positive or negative. Table III contains typical examples of these elements. It is apparent that the principle correlations occur between α and $< v_N>$ and between β and $<v_c>$. In addition, significant correlation also occurs between α and $<v_c>$ and between $<v_N>$ and $<v_c>$. Because of these significant correlations, the effective percent errors on β, $<v_N>$, and $<v_c>$ are usually similar to those quoted above for α. The only exception to this arises when the chosen dead function, f_d, happens to fit the experimental dead function rather poorly. When this happens the fit routine compensates by generating a defective function with a very small value for $<v_c>$. In such cases, which amounted to about 10% of the samples studied, the values of β and $<v_c>$ were meaningless.

TABLE III

PARAMETER CORRELATION MATRIX

	α	β	$<v_N>$	$<v_c>$
α	1.000	0.008	−0.974	−0.218
β	0.008	1.000	−0.078	−0.956
$<v_N>$	−0.974	−0.078	1.000	0.281
$<v_c>$	−0.218	−0.956	0.281	1.000

TABLE IV

FIT PARAMETERS FOR THE EXPERIMENTAL FUNCTIONS NUMBERED IN FIG. 4

Parameter	1	2	3	4
α	0.75	0.28	0.05	0.15
$<v_N>, \mu m/s$	370	310	70	380
β	0.0	0.49	0.50	0.01
$<v_c>, \mu m/s$	0.0	230	69	240
Sum of squares	6.6×10^{-4}	7.7×10^{-4}	4.6×10^{-4}	2.0×10^{-4}

RESULTS AND DISCUSSION

Fig. 4 shows the experimental functions, $g^{(1)}(\tau)$ and corresponding fits (using f_{NL} for f_N in Eq. 9 for 4 of the 88 semen samples studied. These examples were chosen because they demonstrate the sizable differences in the shape of $g^{(1)}(\tau)$ observable from bull spermatozoa preparations. The fit parameters for these four examples are given in Table IV. Table V contains the statistical information on all 88 samples. The values of each parameter appeared to be distributed normally over the samples (eg. Fig. 5) so that standard deviations are also quoted. In general there was considerable variation in α and β from sample to sample, although their average values and standard deviations were similar. It was reassuring to note that whenever a considerable number of circular swimmers was noticed by microscopic examination, the value of β was 0.4 or higher. In many cases, our estimates of the fraction of circular swimmers were higher than the technicians' visual estimates. We are unaware of all the factors that cause the defective swimming, but it is possible that the high dilution that we require is one of them. This possibility deserves more investigation. The average value of the percent motile ($(\alpha + \beta)$ 100) of 53.5% is a bit lower than the figure of 65% motile determined by visual inspection of many samples. However, the light scattering average really should be interpreted as percent particles motile since some large fat globules are present in the semen and add to the dead component of $g^{(1)}(\tau)$. The values of percent normal and percent defective should also be interpreted in this way. While the concentration of fat globules was low and constant over the 88 semen samples studied here, some semen samples may contain sufficiently high concentrations of globules or bac-

TABLE V

AVERAGE VALUES AND STANDARD DEVIATIONS FOR THE FIT PARAMETERS, BASED ON 88 SEMEN SAMPLES

Parameter	Average value	SD
α	0.29	0.17
β	0.24	0.16
$\alpha + \beta$ (fraction alive)	0.53	0.21
$<v_N>, 7 \mu m/s$	384	110
$<v_c>$	103	83

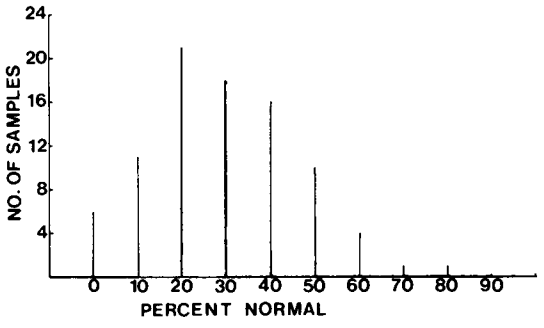

FIGURE 5

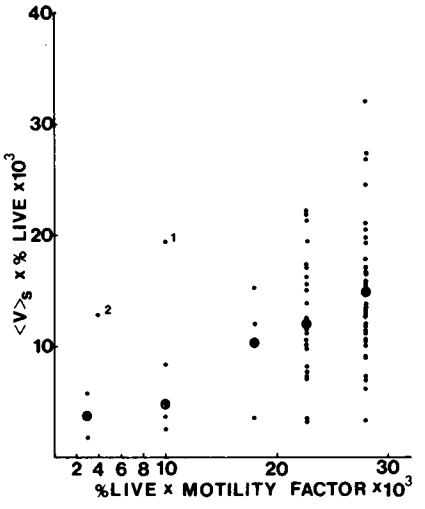

FIGURE 6

FIGURE 5 Distribution of normal swimmers as determined by light scattering for the 88 samples examined.

FIGURE 6 A comparison of semen quality determinations. Light scattering results versus visual observations by the artificial insemination industry technicians.

teria to sizably distort the values of α and β. Thus samples should always be examined via a microscope to check this possibility.

The swimming speeds listed in Table IV are the average trajectory speeds of the cells. To compare the values with those obtained by other techniques, it is first necessary to convert these speeds to translational speeds. Assuming typical values for the pitch and radius of the helical trajectory of 10 μm and 3 μm (Rikmenspoel, 1965) leads to a conversion factor of 0.47 between the helical path and the translational path. Since defective cells move in sinusoidal trajectories about circles of varying radii, it is more difficult to produce a single factor for determining corresponding translational speeds. In addition detailed information of the sinusoidal track is very limited. Microscopic observation of the cells allowed at least a visual comparison between the normal and defective trajectories. The wavelength of the defective trajectory seemed about the same as the pitch of the normal helix. However, the amplitude of the sinusoidal trajectory appeared to be about one half the radius of the normal helix. Using these values, we obtained a conversion factor of 0.83. These factors and the relative populations were considered when the average translation speed of all live cells in a sample was determined. While the absolute values of the translational speeds may be in error because of errors in the conversion factors, relative values are still meaningful.

The average swimming speed of all motile cells in the samples was 260 μm/s. The corresponding average translational speed was found to be 140 μm/s. This average is slightly higher, but still comparable with average speeds estimated by other techniques (Rikmenspoel et al., 1960, 1973; Rikmenspoel, 1963, 1965; Katz and Dott, 1975). The

helical speeds measured for the normal cells in each sample were usually quite close to their average value of 384 μm/s. This average helical speed leads to an expected average translational speed of 180 μm/s. This also seems slightly high. However, the samples used in this study were only about 15 min old and may well be more active. Furthermore, it is difficult to know if the averages quoted by others were for normals only, for motile cells, or for all cells in the sample. The average speed of the circular swimmers was considerably below that of the normals. The average translational speed of these cells was found to be 86 μm/s, similar to estimates from cinematographic observations (Rikmenspoel, 1960).

In order to compare the light scattering results with those obtained by the United Breeders technicians for the same samples, we evaluated the product, percent live, $(\alpha + \beta)$ 100, times the average translational speed for each sample. This product was chosen because it is comparable to the product of two quantities measured by the United Breeders Technicians (percent live $\times$ motility factor). The motility factor is a number from 1 to 5, which the semen-processing industry uses to rate samples. Samples having better motility are given higher factors. Both these parameters were obtained by subjective visual evaluation of the sample through a microscope. Most samples rated a percent live of 65 or 70 and a motility factor of value 3.5 or 4.0. The light scattering and visual parameters are plotted against each other in Fig. 6. While the averages of the data of each vertical group follow a straight line reasonably well and demonstrate a good overall correlation, there is considerable uncertainty on the comparison for any one sample. This is not surprising, however, in view of the large uncertainties associated with the visual evaluation of samples. The numbered data points in Fig. 6 were not used in the averaging procedure that led to the open circle points. These two samples were rated very low by the technicians because they had so many circular swimmers. The light scattering results concurred with this, in that β was found to be about 0.5 (50% circular swimmers) in each case. However, about 40% of the sample in each case were found to be normal swimmers, giving the reasonably high numbers on the light scattering scale of the figure.

CONCLUSION

In this study we have attempted to provide further evidence that quasi-elastic light scattering is a powerful tool for investigating the swimming properties of free suspensions of spermatozoa. The experimental electric field autocorrelation function appears to be composed of three parts, due to normal swimming cells, circular swimming cells, and dead cells. The data indicates that the speed distribution functions for normal swimmers and defective swimmers are gamma distributions with two and one degrees of freedom, respectively. The physical reasons for this are unknown at the present time, although some models of flagellar motion may be consistent with these distributions. The problem certainly deserves considerable effort, both experimental and theoretical.

We would like to thank United Breeders Inc. of Guelph, especially Mr. C. Abreo, for the time and inconvenience associated with this research project. We would like to acknowledge many valuable discussions

with Dr. G. Renninger, Dr. P. A. Egelstaff, Dr. B. Nickel, Dr. G. Hines of the University of Guelph, and Dr. H. Lekkerkerker of the University of Brussels.

We would like to acknowledge the National Research Council of Canada and the Ontario Ministry of Agriculture and Food for their support of this research.

Received for publication 23 September 1977 and in revised form 18 November 1977.

REFERENCES

ADAM, M., A. HAMELIN, P. BERGÉ, and M. GOFFAUX. 1969. Possibilité d'application de la technique de diffusion inélastique de la lumière a l'étude de la vitalité des spermatozoïdes de taureaux. *Ann. Biol. Anim. Biochim. Biophys.* **9**:651–655.

BAIRD, D. C. 1962. Experimentation: An Introduction to Measurement Theory and Experimental Design. Prentice-Hall, Inc., Englewood Cliffs, N.J. 57.

BERNE, B., and R. NOSSAL. 1974. Inelastic light scattering by large structured particles. *Biophys. J.* **14**:865–880.

BERNE, B., and R. PECORA. 1976. Dynamic Light Scattering. John Wiley and Sons, Inc., New York, 376 pp.

BOON, J. P., R. NOSSAL, and S.-H. CHEN. 1974. Light scattering due to wiggling motions of bacteria. *Biophys. J.* **14**:847–864.

BOX, G. P., and G. M. JENKINS. 1970. Time Series Analysis; Forecasting and Control. Holden-Day, Inc., San Francisco, Calif. 575 pp.

BREIMAN, L. 1973. Statistics: with a View toward Applications. Houghton Mifflin Company, Boston, Mass. 25.

CHEN, S.-H., M. HOLZ, and P. TARTAGLIA. 1977. Quasi-elastic light scattering from structured particles. *Appl. Opt.* **16**:187–194.

COMBESCOT, R. 1970. Diffusion d'un rayonnement laser par des spermatozoïdes. *J. Phys. (Paris).* **31**:767–769.

COOKE, D., F. R. HALLETT, and C. A. V. BARKER. 1976. Motility evaluation of bull spermatozoa by photon correlation spectroscopy. *J. Mechanochem. Cell Motility.* **3**:219–223.

DUBOID, M., P. JOUANNET, P. BERGÉ, B. VOLOCHINE, C. SERRES, and G. DAVID. 1975. Méthode et appareillage de mesure objective de la mobilité des spermatozoïdes humains. *Ann. Phys. Biol. Med.* **9**:19–41.

GRAY, A. L., F. R. HALLETT, and A. RAE. 1975. Digital autocorrelation by minicomputer. *J. Phys. E. Sci. Instrum.* **8**:501–506.

JOUANNET, P., B. VOLOCHINE, P. DEGUENT, C. SERRES, and G. DAVID. 1977. Light scattering determination of various characteristic parameters of spermatozoa motility in a serie of human sperm. *Andrologia*. **9**: 36–49.

KATZ, D. F., and H. M. DOTT. 1975. Methods of measuring swimming speeds of spermatozoa. *J. Reprod. Fertil.* **45**:263–272.

NOSSAL, R. 1971. Spectral analysis of laser light scattered from motile microorganisms. *Biophys. J.* **4**:341–354.

NOSSAL, R., S.-H. CHEN, and C. C. LAI. 1971. Use of laser scattering for quantitative determinations of bacterial motility. *Opt. Commun.* **4**:35–39.

NOSSAL, R., and S.-H. CHEN. 1972. Light scattering from motile bacteria. *J. Phys. (Paris).* **33**:C1 171–176.

NOSSAL, R., and S.-H. CHEN. 1972. Laser measurements of chemotactic response of bacteria. *Opt. Commun.* **5**:117–122.

NOSSAL, R., and S.-H. CHEN. 1973. Effects of chemoattractants on the motility of *Escherichia coli*. *Nat. New Biol.* **244**:253–254.

POWELL, M. J. D. 1965. A method for minimizing a sum of squares of non-linear functions without calculating derivatives. *Comput. J.* **7**:303–307.

RIKMENSPOEL, R. 1963. Electronic analyzer for measuring velocity and concentration of spermatozoa. *Rev. Sci. Instrum.* **35**:52–57.

RIKMENSPOEL, R. 1965. The tail movement of bull spermatozoa; observations and model calculations. *Biophys. J.* **5**:365–392.

RIKMENSPOEL, R., G. VAN HERPEN, and J. EIJKHOUT. 1960. Cinematographic observations of the movements of bull sperm cells. *Phys. Med. Biol.* **5**:167–181.

RIKMENSPOEL, R., A. C. JACKLET, S. E. ORRIS, and C. B. LINDEMANN. 1973. Control of bull sperm motility. Effects of viscosity, KCN and thiourea. *J. Mechanochem. Cell Motility.* **2**:7–24.

SCHAEFER, D. W. 1973. Dynamics of number fluctuations: motile microorganisms. *Science (Wash. D. C.).* **180**:1293–1295.

SCHAEFER, D. W., and B. BERNE. 1975. Number fluctuation spectroscopy of microorganisms. *Biophys. J.* **15**:785–794.

SEARLE, S. R. 1971. Linear Models. John Wiley and Sons, Inc., New York. 532 pp.

SHIMIZU, H., and G. MATSUMOTO. 1977. Light scattering on motile spermatozoa. Inst. Elect. Electron. Eng. *(I.E.E.E.) Trans. Biomed. Eng.* **24**:153–157.

WINKLER, R. L., and W. L. HAYS. 1975. Statistics; Probability, Inference and Decision. Holt, Rinehart & Winston, New York. 889 pp.